

The KT phase transition and the XY model

physics760 - Computational physics

Lennart Voorgang

March 27, 2025

Contents

1. Introduction	1
2. Numerical Methods	1
2.1. Monte Carlo Metropolis-Hastings Algorithm	2
2.2. Autocorrelation	2
2.3. Thermalization and Blocking	3
2.4. Bootstrap Analysis	3
2.5. Temperature Scanning	3
2.6. Distributed Computing	4
3. Results	4
3.1. Observables	4
3.1.1. Energy per Spin	4
3.1.2. Magnetization per Spin	5
3.1.3. Specific Heat per Spin	6
3.1.4. Magnetic Susceptibility per Spin	6
3.2. Critical Temperature T_C	7
3.3. Vortex Unbinding	9
3.4. Performance	11
3.4.1. Scheduling	11
3.4.2. Lattice Scaling	11
3.4.3. Critical slowing down	11
4. Conclusion	11
A. Source Code	I
B. Vortex Unbinding	II
List of Figures	III
References	IV

1. Introduction

The perhaps most well known model for the magnetization of lattice structures is the Ising spin model. It describes the total magnetization of a lattice as the superposition of all spins $\sigma_i = \pm 1$ on the lattice.

XY model One can now go and generalize the problem from a \mathbb{Z}_2 symmetry to a continuous $U(2)$ symmetry. This model is called the XY model and describes the spins as two dimensional vectors on the unit circle

$$\sigma_i = \begin{pmatrix} \cos \theta_i \\ \sin \theta_i \end{pmatrix} \quad (1)$$

parametrized by the angle $\theta_i \in [0, 2\pi)$. The Hamiltonian for this system is thus given as

$$H = -J \sum_{\langle i,j \rangle} s_i \cdot s_j = -J \sum_{\langle i,j \rangle} \cos(\Delta\theta) \quad (2)$$

Kosterlitz and Thouless (1973, p. 1190, eq. (42)) where $\Delta\theta = \theta_i - \theta_j$ is the angle between two spins and $J > 0$ the interaction strength. The $\langle i,j \rangle$ notation is used to indicate a nearest neighbour approximation. The partition sum for such a system is given by

$$Z = \sum \exp(-\beta H) \quad (3)$$

where $\beta = (k_B T)^{-1}$ and k_B being the Boltzmann constant. For the remainder of the project we set $J = 1 \text{ J} k_B^{-1}$ such that $\beta = T^{-1}$ is dimensionless.

KT phase transition Unlike the Ising model, the XY model does not have a 2nd order phase transition “as the ground state is unstable against low-energy spin-wave excitations” (Kosterlitz and Thouless (1973, p. 1190)). It does however have something we call KT phase transition where below a critical temperature T_C a metastable state can exist. These metastable states are “corresponding to vortices which are closely bound in pairs” (Kosterlitz and Thouless (1973, p. 1190)) and which come closer together with decreasing temperature until they pair annihilate.

2. Numerical Methods

To get an estimate for the critical temperature and make the vortex pairs visible, we will be using numeric Monte Carlo simulations running on a cluster of CPU nodes. *Rust*¹ was chosen as a fitting programming language for this project, as we want to parallelize the computational effort and the *rust* ownership model makes thread-safe access to data easy.

¹<https://www.rust-lang.org/>

2.1. Monte Carlo Metropolis-Hastings Algorithm

The fundamental problem we need to solve is that we want to generate configurations of our system with probability $P(\sigma) = \exp(-\beta H[\sigma])/Z$. The problem here is that the partition sum Z is not easy to calculate. As shown by Metropolis et al. (1953), it is sufficient to calculate the ratio of probabilities

$$\frac{P(y)}{P(x)} = \exp(-\beta(H[y] - H[x])) = \exp(-\beta\Delta H). \quad (4)$$

This generates a Markov chain of dependent configurations. The overall procedure for the lattice is as follows

1. Calculate E and M for the initial lattice configuration.
2. Perform a lattice sweep by iterating over all lattice sites. For every site i do:
 - a) Propose a new angle $\theta_i \in [0, 2\pi]$ from a uniform distribution.
 - b) Calculate $\Delta H = \Delta E$ and ΔM for the proposed new state.
 - c) Accept or reject state with probability $P = \min(1, \exp(-\beta\Delta H))$
3. Update the observables $E += \Delta E$ and $M += \Delta M$ and add them to the result set.
4. Repeat from 2. for a total of N sweeps.

2.2. Autocorrelation

The configurations obtained from the aforementioned procedure are each dependent on the configurations preceding them. To get a measure for that correlation one can introduce the autocorrelation

$$C(\Delta t) = \langle (O(t) - \mu_O)(O(t + \Delta t) - \mu_O) \rangle \quad (5)$$

and, to get a size independent measure, the normalized autocorrelation

$$\Gamma(\Delta t) = \frac{C(\Delta t)}{C(0)} \quad (6)$$

with Δt being the step between samples, O an observable and μ_O the mean of that observable. This measure decays exponentially with the timescale τ being the point where samples are no longer correlated

$$\tau = \frac{1}{2} + \sum_{t=1}^T \Gamma(t) \quad (7)$$

where we cut off the summation when it first crosses zero.

2.3. Thermalization and Blocking

To now get iid samples we discard the first $[3\tau]$ values in a thermalization step. We then do a blocking step where we put the remaining samples into chunks of size $\lceil \tau \rceil$ and calculate the mean over each of those chunks. All further processing will use these blocked samples which are now iid.

2.4. Bootstrap Analysis

Since the Metropolis-Hastings algorithm scales with the number of lattices sites, it is computationally impractical to run the Metropolis-Hastings algorithm for long timescales. Given that we have an observable whose iid samples follow an gaussian distribution and we already have “enough” iid samples which cover enough of the possible configuration space, we can then use bootstrapping to generate more samples.

1. Collect B intermediate means by repeating the following:
 - a) Take A random samples from the blocked samples obtained in section 2.3 with replacement.
 - b) Calculate the mean of those samples and add the result to the set of intermediate means.
2. Calculate the final mean and the sample standard deviation of those B intermediate means.

2.5. Temperature Scanning

The expectation is that there is an interesting area near the critical temperature and a more boring area far from it. Using the following procedure we can zoom into the interesting area of the magnetic susceptibility.

1. Divide the temperature interval $T \in (0.0, 3.0]$ into 64 steps with step size ΔT .
2. Run the Metropolis-Hastings algorithm on those 64 discrete temperatures on one thread per value. Increment the iteration count and exit if needed.
3. Find the temperature T where the magnetic susceptibility is maximal.
4. Divide the new temperature interval $T \in (T_{\max} - 3\Delta T, T_{\max} + 3\Delta T]$ into 64 steps with step size ΔT and go to 2.

2.6. Distributed Computing

The temperature scanning described in section 2.5 already allows us to distribute the simulation accross 64 threads on a single node. As we have access to the *FZ Jülich SLURM* cluster for this project, it is natural to try to distribute the computational effort accross multiple nodes.

All nodes have access to a fast shared network volume which can be used for synchronization between nodes. We chose to use a *SQLite* database for storing our results on disk. Since *SQLite* is ACID compliant it is also safe to access over a network share. The procedure now is as follows:

1. When invoking the executable the user can specify which lattice sizes should be simulated. This happens for every process for the *SLURM* batch job.
2. Every process tries to register these lattice sizes in a table. The insertion process is handled that only the first insertion happens and the rest are ignored.
3. During the simulation stage every instance can query the database for a lattice size (in descending order) which is not yet handled by another instance. The ACID compliance of the database can ensure that this step is atomic.
4. The instance simulates the lattice size and writes the results back into the results table.

As an additional integrity measure unique constraints on the tables ensure that every lattice size and temperature combination is not handled twice.

3. Results

The following results were obtained for a run on the *JUSUF*² cluster with 2 nodes and 4 tasks per node. The simulation ran for $N = 1\,200\,000$ sweeps on lattice sizes $L \in \{32, 48, \dots, 272\}$ and the bootstrap parameters were $A = N$ and $B = 200\,000$.

3.1. Observables

3.1.1. Energy per Spin

As the total energy of the system as defined in eq. (1) scales with the number of lattice sites, it is often more insightful to observe the energy per spin

$$E = -\frac{1}{L^2} \sum_{\langle i,j \rangle} \cos(\Delta\theta) \quad (8)$$

²<https://www.fz-juelich.de/en/ias/jsc/systems/supercomputers/jusuf>

which has been plotted in fig. 1.

For low temperatures we have a quasi-ordered state where the spins mostly align. Just like in the Ising model the energy per spin is -2.0 when extrapolating to $T = 0$. With increasing temperature the energy slowly vanishes until it asymptotically approaches 0 for big T .

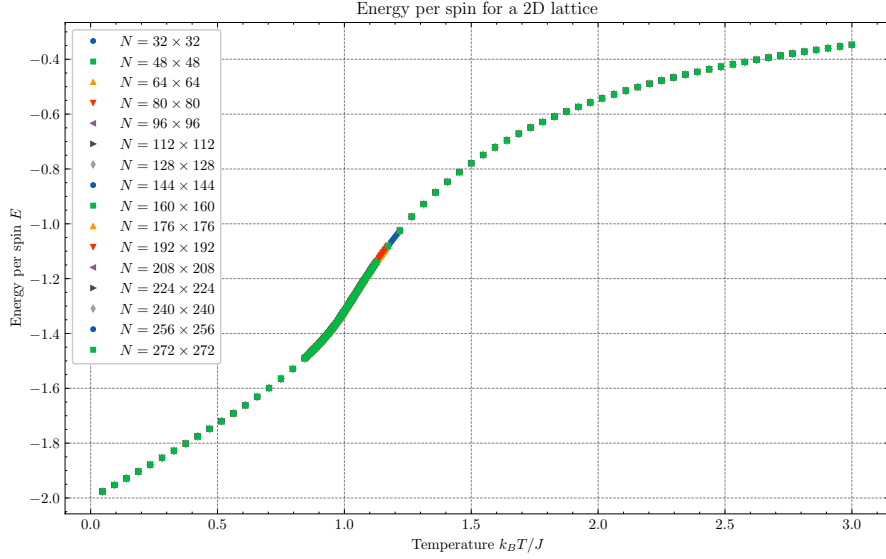


Figure 1: Plot of the temperature dependence of the energy per spin E (eq. (8)) for lattice sizes $L \in \{32, 48, \dots, 272\}$. For small T the energy tends to -2 while for big temperatures the energy asymptotically approaches 0.

3.1.2. Magnetization per Spin

The absolute total magnetization per spin for the system is given by

$$|M|^2 = \frac{1}{L^2} \left(\left(\sum \cos \theta_i \right)^2 + \left(\sum \sin \theta_i \right)^2 \right) \quad (9)$$

and has been plotted in fig. 2.

For low temperature the magnetization tends to 1 which confirms the existence of a quasi-ordered low temperature state. With increasing temperature the magnetization decreases steadily at first and then rapidly until slowly levels out in the unordered high temperature state. One can also see some finite size effects. For increasing lattice sizes the form of the curve becomes more pronounced.

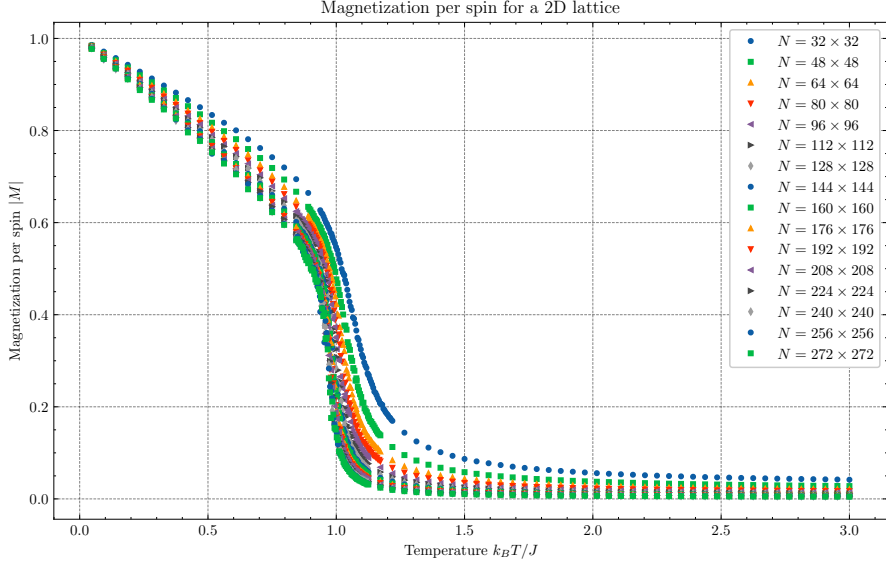


Figure 2: Plot of the temperature dependence of the magnetization per spin $|M|^2$ (eq. (9)) for lattice sizes $L \in \{32, 48, \dots, 272\}$. For small T the magnetization tends to 1 which indicates an ordered state. For big temperatures the magnetization goes to 0 which indicates a unorderd state.

3.1.3. Specific Heat per Spin

The specific heat of the system can be found by evaluating

$$C_V = \frac{\langle E^2 \rangle - \langle E \rangle^2}{T^2} \quad (10)$$

and has bee plotted logarithmically in fig. 3.

The specific heat is small for low temperatures and even smaller for big temperatures. Near the critical temperature there is a small peak which shrinks for increasing lattice sizes. The position of this peak moves towards smaller temperatures when the lattice size is increased.

3.1.4. Magnetic Susceptibility per Spin

The mangetic susceptibility of the system can be found by evaluating

$$\chi = \frac{\langle M^2 \rangle - \langle M \rangle^2}{T} \quad (11)$$

and has bee plotted logarithmically in fig. 4.

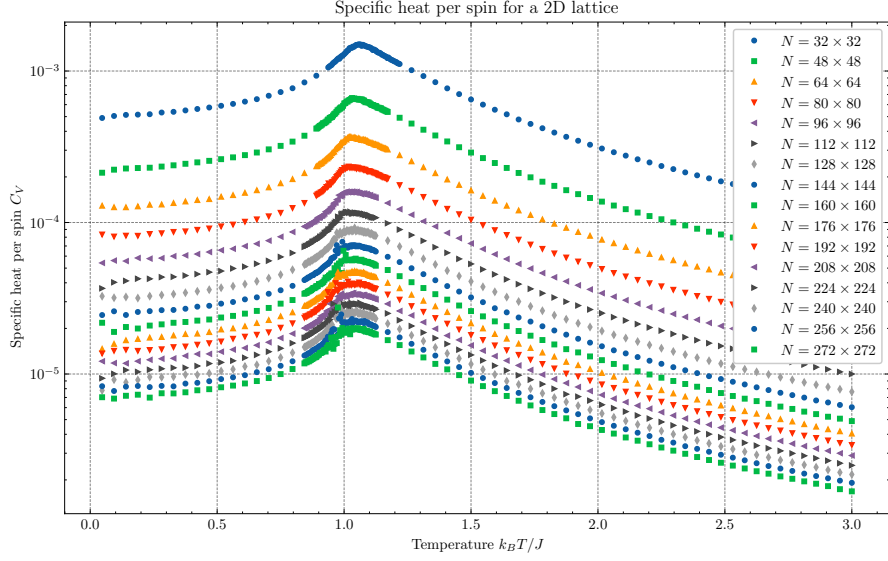


Figure 3: Plot of the temperature dependence of the specific heat per spin C_V (eq. (10)) for lattice sizes $L \in \{32, 48, \dots, 272\}$. The specific heat generally shrinks with increasing lattice size and tends to 0 for very small and big temperatures. There is a peak near the critical temperature T_C which shifts to the left for increasing lattice sizes.

The magnetic susceptibility is small for low and high temperatures. There exists a peak near the critical temperature which slowly moves left and becomes narrower for increasing lattice sizes while the magnitude of the peak slowly shrinks.

3.2. Critical Temperature T_C

To find the critical temperature where the KT phase transition takes place one can use the magnetic susceptibility from section 3.1.4. As shown by Chung (1999) there exists a shifted temperature T^* which asymptotically approaches the critical temperature T_C for an infinite lattice

$$T^*(L) \approx T_C + \frac{\pi^2}{4c(\ln L)^2} \quad (12)$$

(Chung, 1999, eq. 3). To confirm the correlation of lattice size and shifted temperature we now take the maximum magnetic susceptibility χ_{\max} per lattice size from fig. 4 and plot the temperature T where it occurs against $(\ln L)^{-2}$ (fig. 5).

We fitted an ordinary linear regression model using the least square method against our measurements. This fits our data well and confirms the correlation of lattice size and shifted temperature. To estimate our uncertainties we used a parametric bootstrap approach by resampling 10 000 times from our measurements and redoing our linear

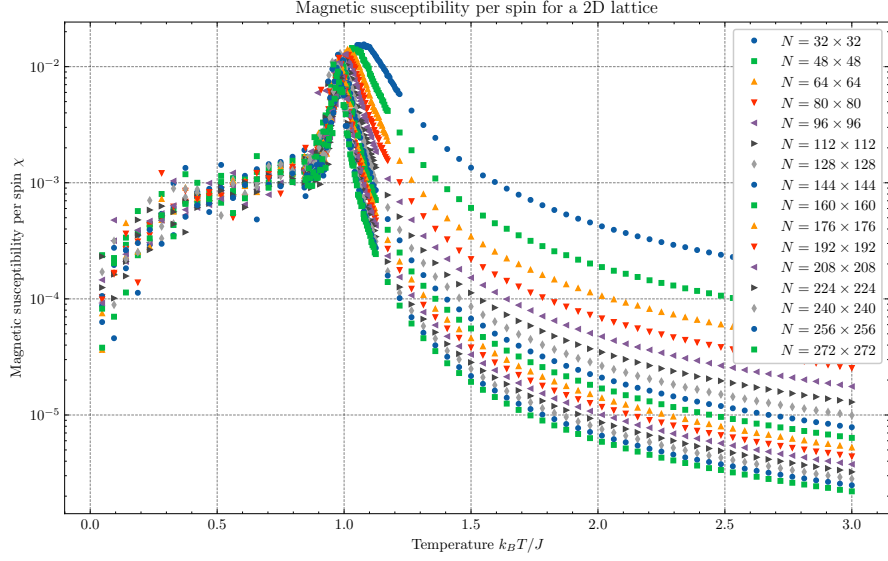


Figure 4: Plot of the temperature dependence of the magnetic susceptibility per spin χ (eq. (11)) for lattice sizes $L \in \{32, 48, \dots, 272\}$. For low and high temperatures the magnetic susceptibility tends towards 0. Near the critical temperature there is a peak which moves left and gets narrower for increasing lattice sizes.

regression model each time. As seen on the right side in fig. 4 the distribution of intercepts b follows a gaussian distribution and therefore the CLT. Taking the standard deviation as the 95 % confidence band we get our estimate for the critical temperature

$$T_C = 0.8941(57). \quad (13)$$

We can now compare our results with some literature values

- In Hsieh et al. (2013) the authors used a GPU based Monte Carlo approach to estimate the critical temperature to $T_C = 0.8935(1)$.
- In Olsson (1995) the authors used a CPU based Monte Carlo approach to estimate the critical temperature to $T_C = 0.89213(10)$.
- A theoretical transfer matrix approach employed by Mattis (1984) lead to a critical temperature of $T_C \approx 0.8916$.

As these estimates lie within the confidence interval of our simulation we may conclude that our simulation was a success. It is of note that our uncertainty is much larger than those of others as we were more constrained by our computational resources and time available.

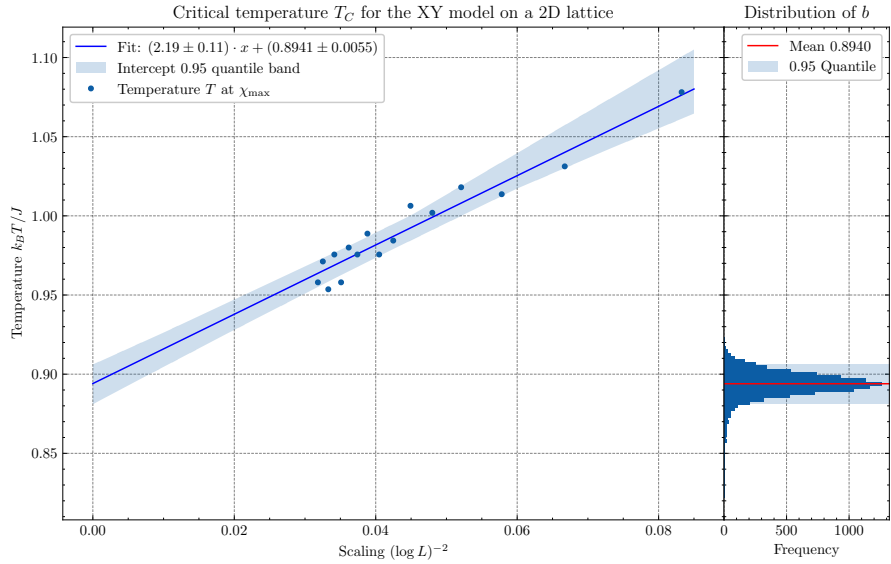


Figure 5: Plotting the temperature from section 3.1.4 at which χ is maximal against $\ln L)^{-2}$ yields a linear correlation. The data was fitted using linear regression model using a least square approach. The uncertainties were estimated using a bootstrap approach. On the right the distribution of intercepts from the bootstrap resampling is plotted.

3.3. Vortex Unbinding

To visualize the vortex unbinding at low temperature we did a singular run where we first heated up a 64×64 lattice to $T = 1.5$ and let it thermalize there for 100 000 sweeps. The temperature was then lowered back down to $T = 0.05$ in 90 steps with 20 sweeps of thermalization at each temperature. At $T = 0.05$ the system was given 90 000 sweeps to let the vortices unbind. An animation of that procedure may be viewed here³ while some of the key frames are shown in fig. 9 of section B.

Below the critical temperature T_C bound vortex / anti-vortex pairs appear. As the temperature further lowered the pairs come closer together until they annihilate. The lattice is left in an quasi-ordered low temperature state.

3.4. Performance

3.4.1. Scheduling

Test

³https://www.youtube.com/watch?v=Gi8mL_0HFxs

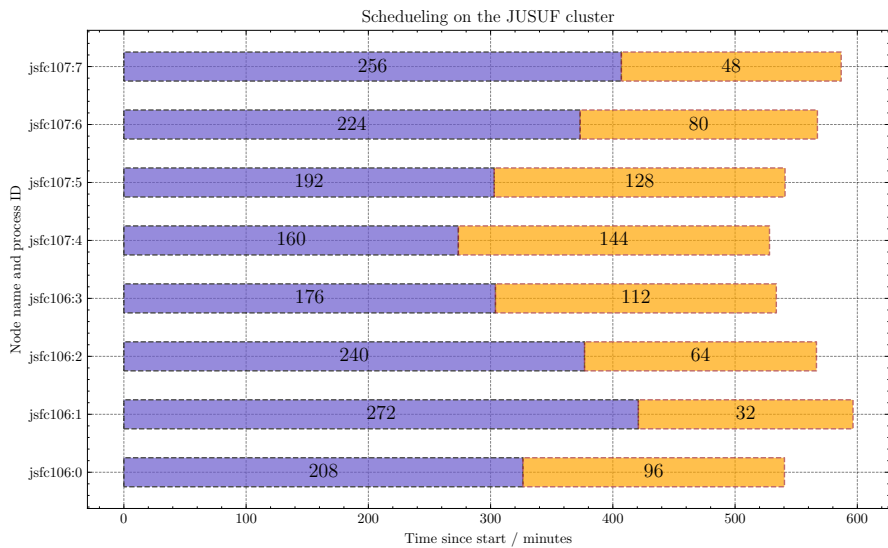


Figure 6: Scheduling

3.4.2. Lattice Scaling

Test

3.4.3. Critical slowing down

Test

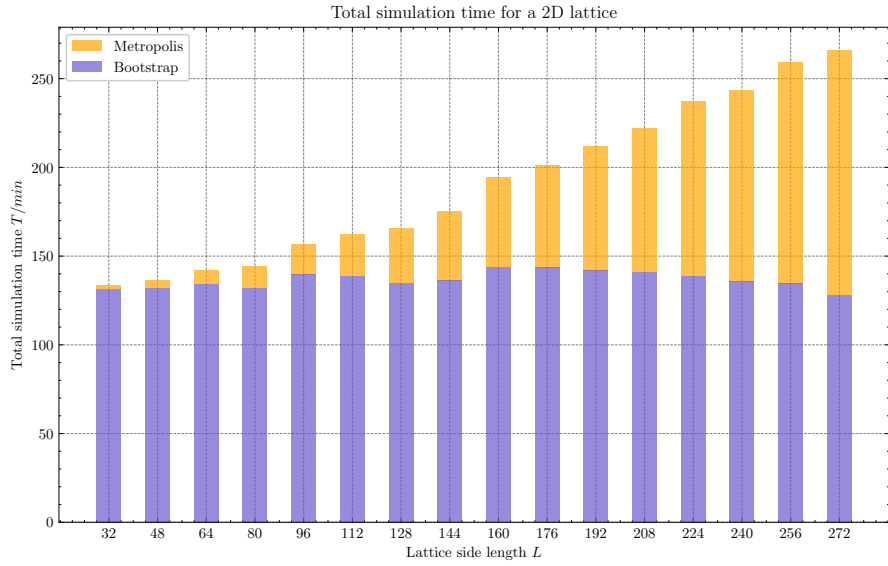


Figure 7: Time scaling

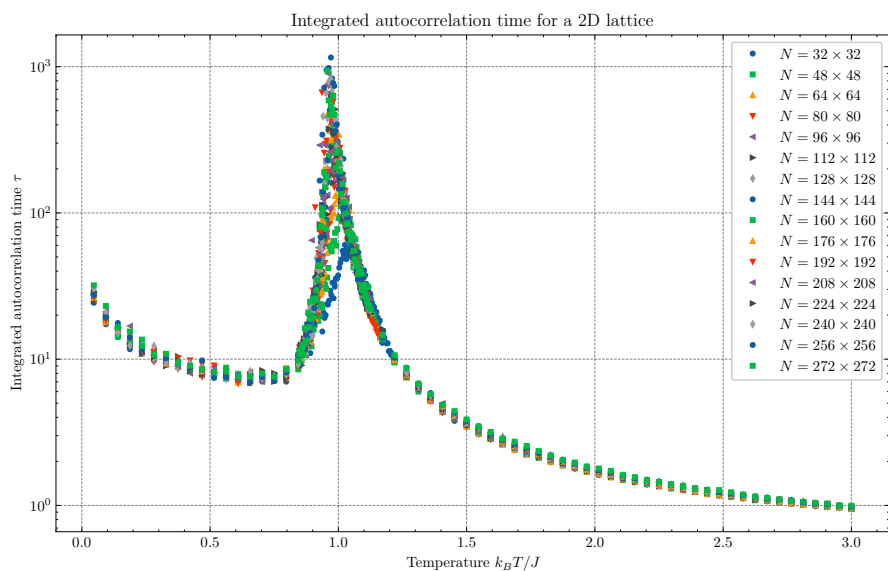


Figure 8: Critical slowing down

4. Conclusion

In this work we were able to simulate the 2D XY model using a numerical Monte Carlo approach. For this we used the Metropolis-Hastings algorithm (section 2.1), bootstrapping (section 2.4) and distributed computing techniques (section 2.6). The simulation ran on the *JUSUF* cluster at *FZ Jülich* and helped us study the observables (section 3.1) energy E , magnetization $|M|^2$, specific heat C_V and magnetic susceptibility χ .

In section 3.2 we used the shifted temperature from eq. (12) to get an estimate for the critical temperature

$$T_C = 0.8941(57). \quad (14)$$

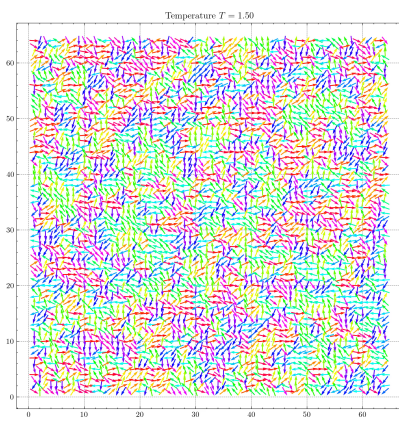
The uncertainty is the 95 % confidence band obtained from bootstrapping the intercept of our linear regression model using a least square algorithm. As discussed in section 3.2 our estimate is compatible with existing literature.

In section 3.3 we observed the existence of bound vortex / anti-vortex pairs below the critical temperature. Further the pair annihilation over long timescales of said vortex pairs was obsererved.

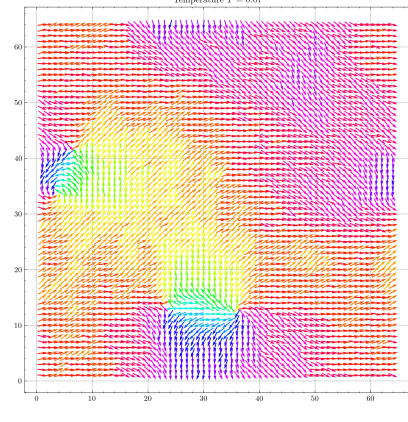
A. Source Code

Test

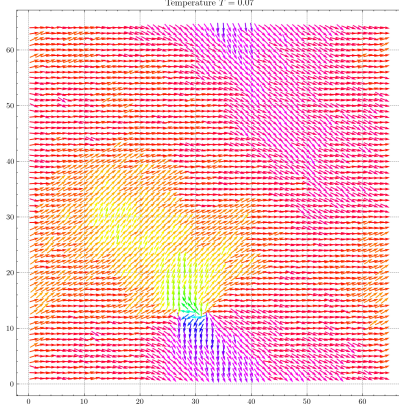
B. Vortex Unbinding



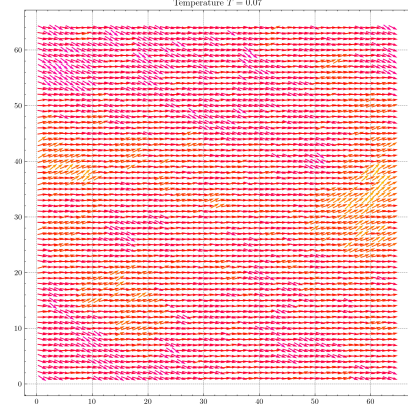
(a) At $T = 1.5$ we are in the high temperature state where there are now vortex pairs and the spins are unordered.



(b) After cooling the system down to $T = 0.05$ there are now two bound vortex pairs and the rest of the spins are aligned.



(c) After some sweeps at $T = 0.05$ the left vortex pair has annihilated while the bottom one has come closer together.



(d) After the second vortex / anti-vortex pair has annihilated we are left with a metastable lattice with ordered spins.

Figure 9: Simulating the process of vortex unbinding by bringing a thermalized high temperature unordered lattice slowly to low temperatures as described in section 3.3. Below the critical temperature T_C bound vortex / anti-vortex pairs appear and slowly annihilate at very low temperatures. The lattice is left in a quasi-ordered low temperature state.

List of Figures

1.	Temperature dependence of the energy per spin E	5
2.	Temperature dependence of the magnetization per spin $ M ^2$	6
3.	Temperature dependence of the specific heat per spin C_V	7
4.	Temperature dependence of the magnetic susceptibility per spin χ	8
5.	Obtaining the critical temperature T_C by plotting the temperature T at χ_{\max} against $(\ln L)^{-2}$	9
6.	Scheduling	10
7.	Time scaling	10
8.	Critical slowing down	11
9.	Vortex unbinding of vortex / antivortex pairs at low temperatures.	II

References

- S. G. Chung. Essential finite-size effect in the two-dimensional xy model. *Phys. Rev. B*, 60:11761–11764, Oct 1999. doi: 10.1103/PhysRevB.60.11761. URL <https://link.aps.org/doi/10.1103/PhysRevB.60.11761>.
- Yun-Da Hsieh, Ying-Jer Kao, and Anders W Sandvik. Finite-size scaling method for the berezinskii–kosterlitz–thouless transition. *Journal of Statistical Mechanics: Theory and Experiment*, 2013(09):P09001, September 2013. ISSN 1742-5468. doi: 10.1088/1742-5468/2013/09/p09001. URL <http://dx.doi.org/10.1088/1742-5468/2013/09/P09001>.
- J M Kosterlitz and D J Thouless. Ordering, metastability and phase transitions in two-dimensional systems. *Journal of Physics C: Solid State Physics*, 6(7):1181, apr 1973. doi: 10.1088/0022-3719/6/7/010. URL <https://dx.doi.org/10.1088/0022-3719/6/7/010>.
- Daniel C. Mattis. Transfer matrix in plane-rotator model. *Physics Letters A*, 104(6):357–360, 1984. ISSN 0375-9601. doi: [https://doi.org/10.1016/0375-9601\(84\)90816-8](https://doi.org/10.1016/0375-9601(84)90816-8). URL <https://www.sciencedirect.com/science/article/pii/0375960184908168>.
- Nicholas Metropolis, Arianna W. Rosenbluth, Marshall N. Rosenbluth, Augusta H. Teller, and Edward Teller. Equation of state calculations by fast computing machines. *The Journal of Chemical Physics*, 21(6):1087–1092, 06 1953. ISSN 0021-9606. doi: 10.1063/1.1699114. URL <https://doi.org/10.1063/1.1699114>.
- Peter Olsson. Monte carlo analysis of the two-dimensional xy model. ii. comparison with the kosterlitz renormalization-group equations. *Phys. Rev. B*, 52:4526–4535, Aug 1995. doi: 10.1103/PhysRevB.52.4526. URL <https://link.aps.org/doi/10.1103/PhysRevB.52.4526>.